Testosterone Protects Against Atherosclerosis in Male Mice by Targeting Thymic Epithelial Cells—Brief Report

Anna S. Wilhelmson, Marta Lantero Rodriguez, Elin Svedlund Eriksson, Inger Johansson, Per Fogelstrand, Alexandra Stubelius, Susanne Lindgren, Johan B. Fagman, Göran K. Hansson, Hans Carlsten, Mikael C.I. Karlsson, Olov Ekwall, Åsa Tivesten

Objective—Androgen deprivation therapy has been associated with increased cardiovascular risk in men. Experimental studies support that testosterone protects against atherosclerosis, but the target cell remains unclear. T cells are important modulators of atherosclerosis, and deficiency of testosterone or its receptor, the AR (androgen receptor), induces a prominent increase in thymus size. Here, we tested the hypothesis that atherosclerosis induced by testosterone deficiency in male mice is T-cell dependent. Further, given the important role of the thymic epithelium for T-cell homeostasis and development, we hypothesized that depletion of the AR in thymic epithelial cells will result in increased atherosclerosis.

Approach and Results—Prepubertal castration of male atherosclerosis-prone apoE^{−/−} mice increased atherosclerotic lesion area. Depletion of T cells using an anti-CD3 antibody abolished castration-induced atherogenesis, demonstrating a role of T cells. Male mice with depletion of the AR specifically in epithelial cells (E-ARKO [epithelial cell-specific AR knockout] mice) showed increased thymus weight, comparable with that of castrated mice. E-ARKO mice on an apoE^{−/−} background displayed significantly increased atherosclerosis and increased infiltration of T cells in the vascular adventitia, supporting a T-cell–driven mechanism. Consistent with a role of the thymus, E-ARKO apoE^{−/−} males subjected to prepubertal thymectomy showed no atherosclerosis phenotype.

Conclusions—We show that atherogenesis induced by testosterone/AR deficiency is thymus- and T-cell dependent in male mice and that the thymic epithelial cell is a likely target cell for the antiatherogenic actions of testosterone. These insights may pave the way for new therapeutic strategies for safer endocrine treatment of prostate cancer.

Visual Overview—An online visual overview is available for this article. (***Arterioscler Thromb Vasc Biol***. 2018;38:1519-1527. DOI: 10.1161/ATVBAHA.118.311252.)

Key Words: androgens ■ atherosclerosis ■ risk factors ■ T-lymphocytes ■ thymus gland

Low testosterone levels in men are associated with increased atherosclerosis burden and increased risk of cardiovascular events.[1,2] Data indicating that castration or androgen deprivation therapy in men with prostate cancer augments cardiovascular risk also support atheroprotective actions performed by testosterone.[3] This notion is further strengthened by experimental studies in which castration, that is, removal of the testes and thereby complete testosterone deficiency, increases atherogenesis and that this effect is abolished by physiological testosterone replacement.[4] Further, depletion of the receptor for testosterone (the AR [androgen receptor]) increases atherosclerosis burden in male mice.[4]

Key steps of the atherosclerotic process include hypercholesterolemia, retention of lipoprotein particles in the vascular wall, activation of endothelial cells, and migration of blood-borne cells into the artery.[5] Macrophages and T cells that accumulate in the arterial intima instigate innate and adaptive immune reactions against lipoprotein-derived molecules.[6] This leads to vascular inflammation and formation of atherosclerotic plaques[5] that may rupture or erode, leading to clinical events. Illustrating the role of vascular inflammation, a large clinical trial recently demonstrated that anti-inflammatory therapy can prevent clinical cardiovascular events.[7]

DOI: 10.1161/ATVBAHA.118.311252

Research performed during the last 2 decades has identified an important, yet complex, modulation of atherogenesis exerted by T lymphocytes.[5] T-cell progenitors are produced in the bone marrow and then enrolled in thymopoiesis, that is, further proliferation and maturation of T cells, in the thymus. It is well known that sex hormones have a crucial impact on thymus size and are responsible for the involution of the thymus taking place during puberty in both mice and humans. In androgen-deficient states, both thymus size and thymopoiesis are prominently increased, and accordingly, the thymus involutes on treatment with androgens.[8–13] However, the potential consequence of this modulation for the pathogenesis of T-cell–dependent disorders, including atherosclerosis, is unknown.

Although considerably less well developed than selective estrogen receptor modulators, the development of compounds that regulate AR activity in a tissue-specific way (selective AR modulators) is ongoing.[14] A crucial step for the design of selective AR modulators with a beneficial cardiovascular profile will be the identification of the target cell(s) for the cardiovascular actions of testosterone. The target cell and mechanism through which androgens/AR protect against atherosclerosis remains unclear[15]; recent studies using cell-specific depletion of the AR do not support endothelial or vascular smooth muscle cells as targets for the antiatherogenic actions of testosterone.[16] Further, contrary to the effects of castration or whole-body AR depletion,[4] monocyte/macrophage-specific AR knockout reduces atherosclerosis.[16]

The aim of the present study was to test the hypothesis that atherosclerosis induced by testosterone deficiency in male mice is T-cell dependent. Further, given the important role of the thymic epithelium for T-cell homeostasis,[17] we hypothesized that depletion of the AR in thymic epithelial cells (TECs) will result in increased atherosclerosis.

Materials and Methods

The data that support the findings of this study are available from the corresponding author on reasonable request.

Animals and Study Design

Male E-ARKO (epithelial cell-specific AR knockout) mice were generated by breeding $AR^{+/flox}$ female mice[18] (from Dr Verhoeven, Katholieke Universiteit Leuven, Belgium) with male K5-Cre+ mice[19] (created by Dr Ramirez, CIEMAT, Madrid, Spain; transferred from Dr Rognoni, Max Planck Institute, Germany). The AR is located on the X chromosome, and male mice with the genotype $AR^{flox/Y}$K5-Cre+/- will become E-ARKO; littermate controls were $AR^{+/Y}$K5-Cre+/-. Assessment of atherosclerotic lesion formation was done in AR^{flox} and K5-Cre+ strains crossed to an apoE constitutive knockout background (B6.129P2-Apoe^tm1UncN11; Taconic), yielding $AR^{flox/Y}$K5-Cre+/- apoE−/− (E-ARKO apoE−/−) and $AR^{+/Y}$K5-Cre+/- apoE−/− (controls). Because our initial assessments of androgen status (wet weight of androgen-sensitive organs), thymus weight and cellularity, and atherosclerotic lesion formation (data not shown) revealed no differences between AR+ and AR^{flox} males, Cre+ littermates without the AR^{flox} construct were used as controls for subsequent experiments. We assessed AR, Cre, and Zfy (for sex) by polymerase chain reaction amplification of genomic DNA.[18] In all experiments, littermate male controls were used, and all mice were on a C57BL/6J background (backcrossed ≥10 generations). The mice were housed in a temperature- and humidity-controlled room with a 6- to 18-hour light cycle and consumed a soy-free chow diet (Cat No. R70; Lantmännen) and tap water ad libitum. All animal studies were conducted in compliance with local guidelines, and the Ethics Committee on Animal Care and Use in Gothenburg approved all procedures. The studies adhere to the American Heart Association recommendations for experimental atherosclerosis studies[20]; deviations include that no statistical methods were used to predetermine sample size and that atherosclerosis was assessed at only 1 time point.

Castration (Orchiectomy)

The mice were anesthetized with isoflurane (IsoFlo vet, Vnr 002185; Zoetis) and either sham operated or bilaterally castrated/orchiectomized. Buprenorphine (Temgesic; RB Pharmaceuticals, Ltd) was used for analgesia after all surgical procedures.

Castration and Testosterone Replacement

Four weeks before tissue collection, 8-week-old male C57BL/6J mice were bilaterally castrated and implanted subcutaneously with a small slow-releasing pellet containing vehicle/placebo (Cat No. SC-111) or a physiological dose of testosterone[4] (25 µg/d; Cat No. SA-151; Innovative Research of America, Sarasota, FL).

T-Cell–Depletion Experiment

At 4 weeks of age, male apoE-deficient mice (B6.129P2-Apoe^tm1UncN11; Taconic) were bilaterally castrated or sham operated under isoflurane anesthesia. One week later, the mice were injected intraperitoneally with 50 µg anti-mouse CD3 antibody (clone 145-2C11 f[ab′]2 fragments, Cat No. BE0001-1FAB; BioXCell) or a control antibody (hamster IgG f[ab′]2 fragments, Cat No. BE0091-FAB; BioXCell) on 5 consecutive days. As described previously,[21] the antibody injections were repeated with 3-week intervals (when the mice were 5, 8, 11, and 14 weeks of age), and the mice were euthanized at 16 weeks of age.

Thymectomy Experiments

At 3 weeks of age, male apoE-deficient mice and apoE-deficient E-ARKO mice and littermate K5-Cre+ controls were thymectomized or sham operated. In brief, mice were anesthetized with isoflurane, thymus exposed via a suprasternal incision and removed using vacuum aspiration. Completeness of the thymectomy was ensured at euthanization at 16 weeks of age.

Tissue Collection

At 16 weeks of age (if not otherwise stated), the mice were anesthetized, blood was drawn from the left ventricle, and the mice were perfused with saline under physiological pressure. Thymus was dissected and kept in PBS on ice. Serum was prepared by clotting of blood in Multivette 600 Z-Gel tubes (Cat No. 15.1674; Sarstedts) and separated by centrifugation. The serum was subsequently frozen at −80°C.

Histological Analyses in the Aortic Root

Serial 10-µm cryosections were cut distally from the aortic root. Sections at 200, 400, 600, and 800 µm after the appearance of the aortic cusps were stained with Oil Red O (Cat No. 00625; Sigma-Aldrich) and counterstained with hematoxylin. Staining with Masson trichrome was performed according to the manufacturer's instructions (Accustain Trichrome Stains-Masson, Cat No. HT15; Sigma-Aldrich). Other sections were stained for macrophages using a rat anti-mouse Mac-2 antibody-FITC (fluorescein isothiocyanate)–conjugated (M3/38; Cedarlane; 1:1000, 0.1 µg/mL), followed by a secondary mouse anti-FITC-biotin–conjugated antibody (FL-D6; Sigma; 1:1000, 3 µg/mL). Staining was detected using an alkaline phosphate system (Cat No. AK-5000; Vector Laboratories, Inc) and developed

with Vulcan fast red (Cat No. BC-FR805S; Biocare Medical). For immunofluorescence, sections were incubated with rat anti-mouse CD18 (C71/16; Biolegend; 1:100, 10 µg/mL), mouse anti-smooth muscle α-actin-Cy3 (1A4; Sigma-Aldrich; 1:10 000, 0.2 µg/mL), and hamster anti-mouse CD3e (145-2C11; eBioscience; 1:100, 5 µg/mL), followed by secondary antibodies: AF647-conjugated donkey anti-rat IgG (Cat No. 712-606-153; Jackson Immuno Research Laboratories; 1:300, 5 µg/mL) and AF594-conjugated goat anti-hamster IgG (Cat No. 127-585-160; Jackson Immuno Research Laboratories; 1:300, 5 µg/mL) and staining with DAPI (4',6-diamidino-2-phenylindole; Cat No. D9542; Sigma-Aldrich).

We used morphometric analysis (BioPix Software) to determine the size of the atherosclerotic lesions and the adventitia, after manual delineation. As an estimate of atherosclerotic lesion size, atherosclerotic lesion areas at the levels 200, 400, 600, and 800 µm from the aortic cusps were integrated. The areas of Mac-2 staining and collagen staining (blue color in Masson trichrome) were determined using Biopix Software; thresholds were defined manually by a blinded observer and applied equally to all stained sections. The number of anti-CD3–stained cells was manually counted and normalized to lesion and adventitia area, respectively. All evaluations of aortic root sections were performed by a blinded observer.

Thymus Sections

Ten-micrometer cryosections were cut throughout the thymus, and sections were stained by hematoxylin (Cat No. 1820; Histolab) and eosin (Cat No. ACRO409430250; VWR). The section with the largest thymic lobe area was identified for each mouse and further used for manual delineation of the thymic medulla and cortex (BioPix Software) by a blinded observer.

Cell Preparation and Flow Cytometry Analysis of T Lymphocytes

Single cells from spleen and thymus were prepared by passing the tissue through a 70-µm cell strainer (Cat No. 10788201; Thermo Fisher) using PBS and a syringe plunger. Erythrocytes in spleen and whole blood were lyzed in 0.16 mol/L NH_4Cl, 0.13 mol/L EDTA, and 12 mmol/L $NaHCO_3$; the cells were washed in flow cytometry buffer (2% fetal bovine serum and 2 mmol/L EDTA in PBS) and counted in an automated cell counter (Sysmex). After FcR blockage (anti-mouse CD16/CD32; BD Biosciences; 1:100, 5 µg/mL), antibodies specific for the following molecules were used: CD4 (GK1.5; Biolegend; 1:100, 2 µg/mL) and CD8a (53–6.7; eBioscience; 1:100, 2 µg/mL). Immunostained cells were analyzed on a FACS Canto II or Accuri C6. All instruments were from Becton Dickinson. Data were analyzed using FlowJo (Tree Star) and fluorochrome minus one staining was used as controls.

Cell Preparation and Flow Cytometry Sorting of TECs

The thymi were fragmented and excess of thymocytes washed away by mechanical disruption. TECs were released by enzymatic digestion. Briefly, the thymic fragments were incubated in digestion medium: 0.5 U/mL Liberase (Cat No. 5401127001; Roche), 0.2 mg/mL DNase I (Cat No. 11284932001; Roche) in DMEM/F12 at 37°C with gentle mixing for 20 minutes. The released cells were transferred into cold flow cytometry buffer. New prewarmed digestion medium was added to remaining thymic fragments for 2 more consecutive incubations, to completely dissolve the tissue. The released cell fractions were filtered through a 100-µm cell strainer (BD Biosciences), washed, and counted. Cells from the 2 latter fractions were pooled and used for cell sorting. After incubation with FcR block (CD16/CD32; BD Biosciences; 1:100, 5 µg/mL), antibodies against CD45 (30-F11; BD Biosciences; 1:200, 0.5 µg/mL) and EpCAM (epithelial cellular adhesion molecule)/CD326 (G8.8; BD Biosciences; 1:300, 0.7 µg/mL) were added. The cells were washed, resuspended in flow cytometry buffer to 10^7 per mL, and filtered through a 100-µm cell strainer. TECs (CD45⁻ EpCAM⁺) were sorted on a SY3200 cell sorter (SONY Biotechnology, Inc).

AR DNA Quantification

In the ARKO mouse model, exon 2 of the AR gene is excised,[18] and the presence of exon 2 versus exon 3 was used to quantify the efficacy of the AR knockout. CD3⁺ cells were isolated from thymus using positive selection with MACS (magnetic-activated cell sorting) CD3 microbeads (Cat No. 130-094-973; Miltenyi Biotec). Genomic DNA from CD3⁺ cells and TECs (sorted as described above) was isolated using DNeasy blood and tissue kit (Cat No. 69504; Qiagen) according to the manufacturer's instructions. Genomic DNA amplification was detected using SyBR green master mix (Cat No. 4367659; Applied Biosystems) in an ABI Prism 7900HT Sequence Detection System (Applied Biosystems). The following primer pairs were used: AR exon 2, forward GGACCATGTTTTACCCATCG and reverse CCACAAGTGAGAGCTCCGTA; and AR exon 3, forward TCTATGTGCCAGCAGAAACG and reverse CCCAGAGTCATCCC TGCTT. Ct values for AR exon 2 were normalized to Ct values for AR exon 3 using the $2^{-\Delta\Delta ct}$ method.[22]

Serum Cholesterol Measurement

Serum total cholesterol and triglyceride levels were determined using Infinity reagents (Cat No. TR13421 and TR22421; Thermo Fisher Scientific), according to the manufacturer's instructions.

Serum Testosterone by Gas Chromatography-Tandem Mass Spectrometry

Serum testosterone levels were determined using an in-house gas chromatography–tandem mass spectrometry assay as described previously.[23]

Statistics

Statistical evaluations were performed with Prism software (GraphPad Software, Inc). All variables were tested for normal distribution (Shapiro-Wilk normality test) and equality of variances (2 groups by F test and 4 groups by Brown-Forsythe test). For variables that passed normality and equal variance tests with or without log transformation, 2-group comparisons were performed by Student *t* test and 4-group comparisons with 2 independent variables by 2-way ANOVA followed by Sidak multiple comparisons test. For repeated measurements, 2-way repeated measurements ANOVA was utilized. Data that did not pass normality or equal variance tests were analyzed using a Mann-Whitney *U* test (2 groups) or Kruskal-Wallis test followed by Mann-Whitney *U* test (4 groups). *P* values of <0.05 were considered statistically significant. Unless otherwise specified, results are represented as mean±SEM.

Results

Increased Thymus Weight and Peripheral T Cells in Testosterone-Deficient Male Mice

We first wished to confirm the effect of castration on thymus weight in male mice. Thymus weight was increased already 5 days after castration of adult mice and was almost doubled after 7 days (Figure 1A). Prepubertal castration resulted in a similar effect on thymus weight, and the effect remained in older mice (Figure 1B). Analyzing gross morphology of the thymus, castration increased areas of both the thymic medulla and cortex (Figure 1C and 1D).

We next asked whether castration affects the peripheral pool of T cells. Indeed, castration increased CD4⁺ T cells in blood and spleen with a similar trend for CD8⁺ T cells (Figure 1E and 1F). Testosterone replacement to castrated mice reduced thymus weight (Figure 1G) and CD4⁺ and CD8⁺ T cells in spleen (Figure 1H).
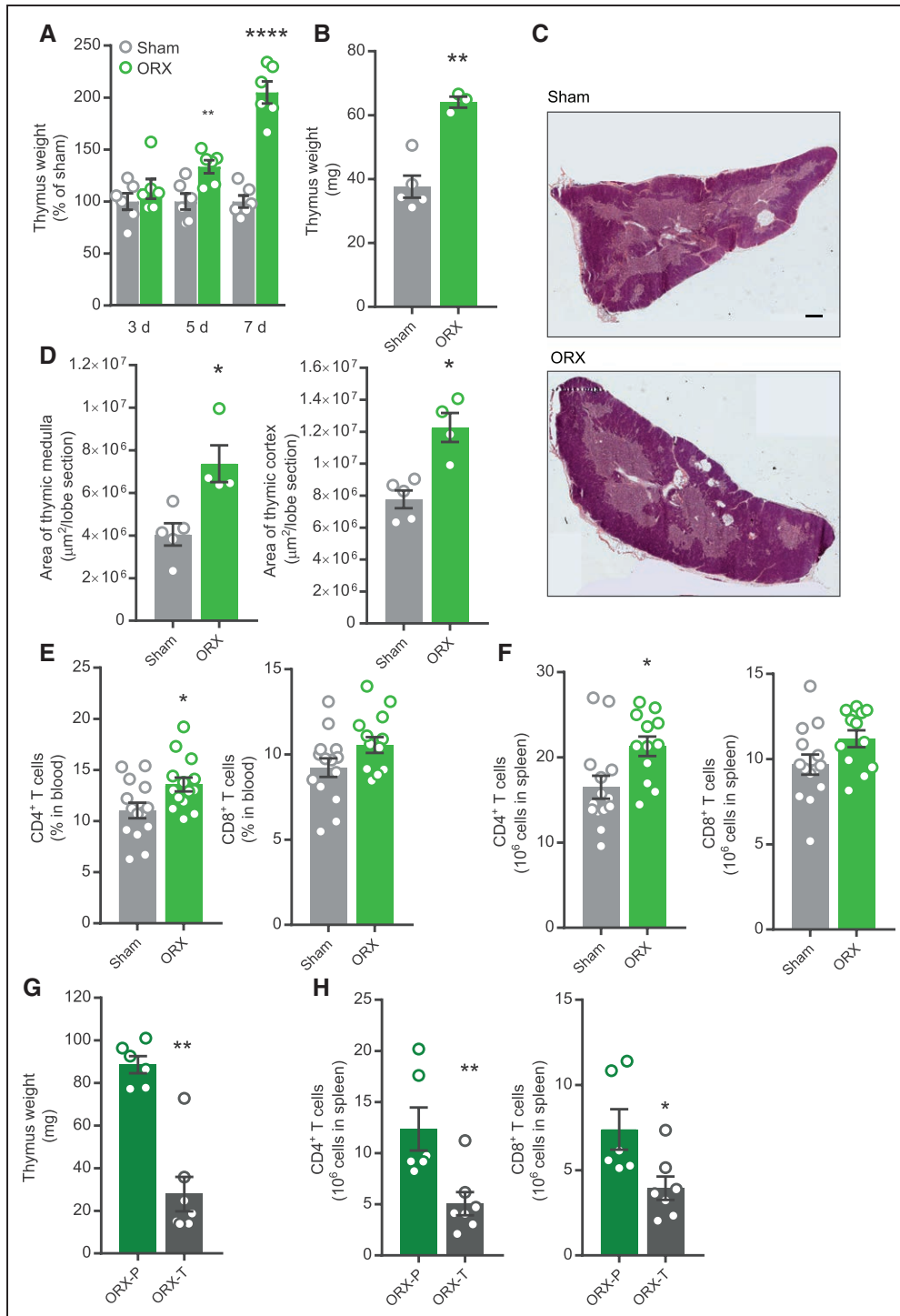
Figure 1. Increased thymus weight and peripheral T cells in testosterone-deficient male mice. **A**, Adult male C57BL/6J mice were ORX (castrated) or sham operated and thymus weight recorded at 3, 5, and 7 d after surgery. **P<0.01, ****P<0.0001 vs corresponding sham group (Student *t* test). n=6 per group. **B–D**, Male apoE$^{-/-}$ mice were sham operated (n=5) or ORX (n=4) at 4 wk of age and thymus collected at 34 wk of age. **B**, Thymus weight. **P<0.01 vs sham group (Student *t* test). **C**, Representative thymus sections from sham-operated and ORX mice, stained by hematoxylin-eosin (scale bar=400 µm). **D**, Quantification of areas of thymic medulla and cortex. *P<0.05 vs sham (Student *t* test). **E**, Male apoE$^{-/-}$ mice were sham operated (n=14) or ORX (n=14) at 4 wk of age and percentage CD4$^+$ and CD8$^+$ T cells in blood analyzed by flow cytometry at 11 wk of age. *P<0.05 vs sham (Student *t* test). **F**, Male apoE$^{-/-}$ mice were sham operated (n=14) or ORX (n=12) at 4 wk of age and CD4$^+$ and CD8$^+$ T cells in spleen analyzed by flow cytometry at 16 wk of age. **P<0.01 vs sham (Student *t* test). **G** and **H**, Male C57BL/6J mice were ORX at 8 wk of age and treated with vehicle (P; n=6) or a physiological testosterone dose (T; n=7) for 4 wk. **G**, Thymus weight at 12 wk of age. **P<0.01 vs sham (Mann-Whitney *U* test). **H**, CD4$^+$ and CD8$^+$ T cells in spleen analyzed by flow cytometry at 12 wk of age. *P<0.05 vs sham (Mann-Whitney *U* test), **P<0.01 vs sham (Student *t* test). Bars indicate means, error bars indicate SEM, and circles represent individual mice.
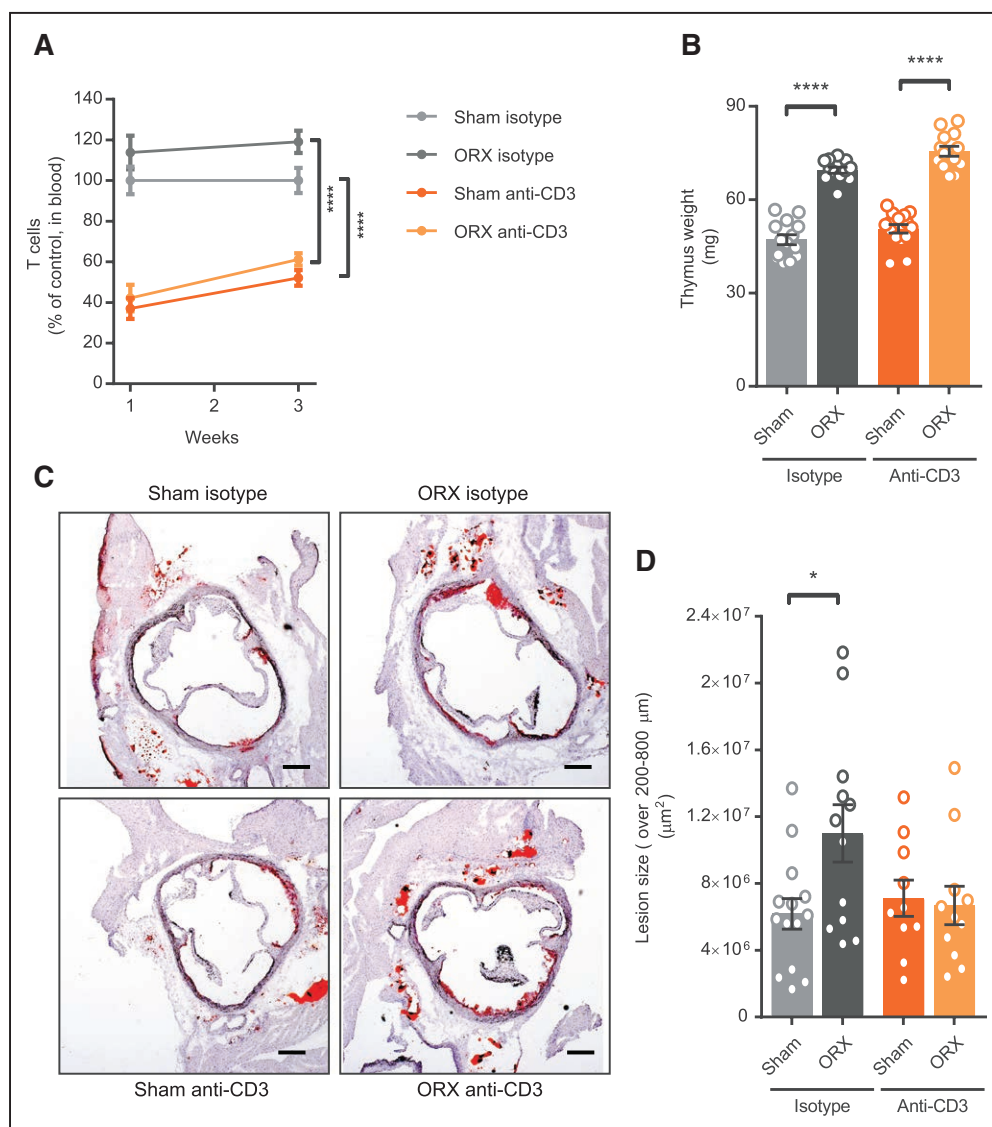
Figure 2. T-cell depletion blocks increased atherogenesis in testosterone-deficient male mice. **A,** Fraction of blood T cells (CD4+ and CD8+) at 1 and 3 wk post-injection of anti-CD3 antibody or isotype control in sham-operated (Sham) or ORX (castrated) male apoE−/− mice (Sham isotype, n=14; ORX isotype, n=14; Sham anti-CD3, n=15; ORX anti-CD3, n=15). Data were analyzed by 2-way repeated measurements ANOVA followed by Sidak multiple comparisons test. ****$P<0.0001$ (effect of antibody treatment in Sham and ORX groups at both time points). **B,** Thymus weight at 16 wk of age in vehicle-treated and anti-CD3–treated sham-operated or ORX male apoE−/− mice fed a normal chow diet (Sham isotype, n=14; ORX isotype, n=12; Sham anti-CD3, n=15; ORX anti-CD3, n=13). Surgery was performed at 4 wk of age and antibody injections given from 5 wk of age, with 3-wk intervals. Data were analyzed by 2-way ANOVA (effect of surgery and antibody treatment; $P<0.01$) followed by Sidak multiple comparisons test (****$P<0.0001$ effect of surgery). **C** and **D,** Atherosclerotic lesion size at 16 wk of age in sections collected at 200, 400, 600, and 800 µm from the aortic cusps (Sham isotype, n=14; ORX isotype, n=12; Sham anti-CD3, n=10; ORX anti-CD3, n=11) and representative pictures of Oil Red O staining of aortic root sections (scale bar=200 µm). Data were analyzed by 2-way ANOVA (interaction; $P<0.05$) followed by Sidak multiple comparisons test (*$P<0.05$ effect of surgery in isotype-treated mice). Bars indicate means, error bars indicate SEM, and circles represent individual mice.

T-Cell Depletion Blocks Increased Atherogenesis in Testosterone-Deficient Male Mice

To test the hypothesis of a role of T cells in castration-induced atherogenesis, we used a T-cell–depleting antibody regimen combined with prepubertal castration or sham surgery of male apoE−/− mice. In blood, the relative number of T cells was reduced by >60% with the antibody treatment as assessed 1 week after injection, and the T-cell depletion was essentially maintained during the 3-week injection interval (Figure 2A). The antibody had a similar effect on the number of T cells in blood in sham-operated and castrated mice (Figure 2A).

There was a similar effect of castration on body weight (Figure IA in the online-only Data Supplement), weight of the androgen-sensitive seminal vesicles (Figure IB in the online-only Data Supplement), and thymus weight (Figure 2B) in isotype and anti-CD3–treated mice. Further, cholesterol levels were not significantly changed by castration or T-cell depletion (Figure IC in the online-only Data Supplement).

Assessing atherosclerosis after 11 weeks of castration/anti-CD3 antibody treatment, we found that the T-cell depletion regimen per se had no effect on atherosclerosis. However, there was an interaction between surgery and antibody
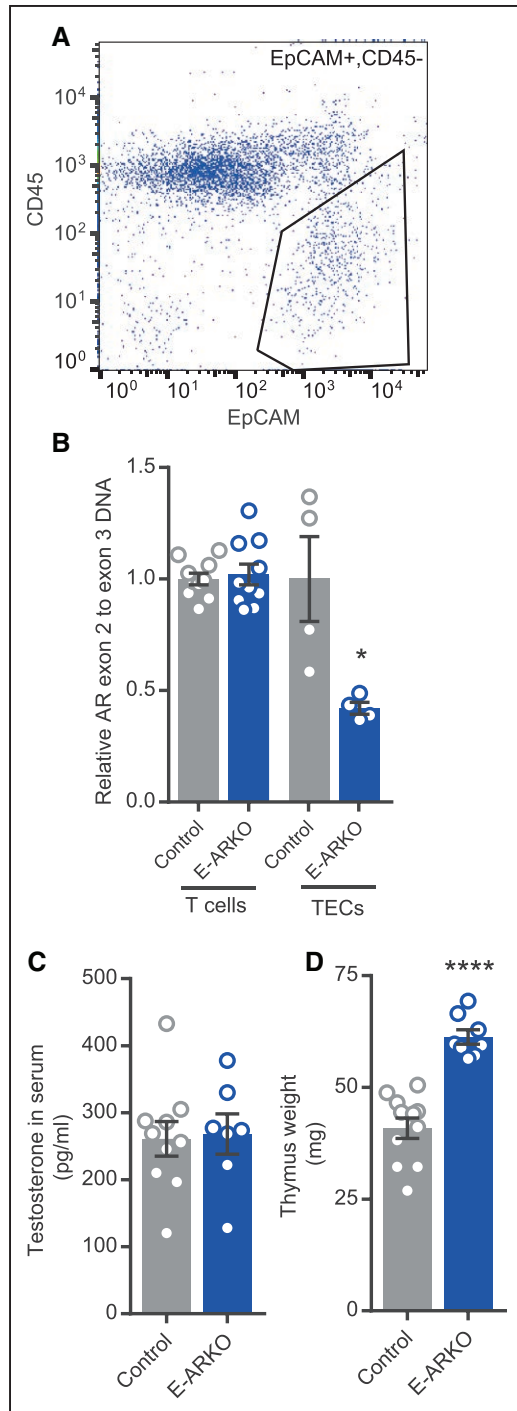
Figure 3. Increased thymus weight in males with depletion of the AR (androgen receptor) in epithelial cells (E-ARKO [epithelial cell-specific AR knockout]). **A**, Gating strategy for sorting thymic epithelial cells (TECs). **B**, Assessment of AR knockout by measurement of exon 2 genomic DNA in control (K5-Cre⁺) and E-ARKO mice, in enriched CD3⁺ T cells from thymus (control, n=10; and E-ARKO, n=10) and sorted TECs (control, n=4; and E-ARKO, n=4). *$P<0.05$ (Mann-Whitney *U* test). **C**, Serum testosterone assessed by gas chromatography–tandem mass spectrometry in 18- to 19-wk-old control (n=10) and E-ARKO mice (n=7). **D**, Thymus weight of control (K5-Cre⁺; n=11) and E-ARKO (n=8) apoE⁻/⁻ mice at 16 wk of age. ****$P<0.0001$ (Student *t* test). Bars indicate means, error bars indicate SEM, and circles represent individual mice.

treatment, such that castration increased atherosclerosis versus sham controls among isotype-treated (mean difference, 4.8×10^6 μm^2; 95% confidence interval, 0.9×10^6 to 8.6×10^6

μm^2) but not anti-CD3–treated (mean difference, -0.4×10^6 μm^2; 95% confidence interval, -3.8×10^6 to 2.9×10^6 μm^2) mice (Figure 2C and 2D).

Increased Thymus Weight in Males With Depletion of the AR in Epithelial Cells (E-ARKO)

As factors secreted by the thymic stroma are known to influence the thymic microenvironment to support T lymphopoiesis[17] and the AR is expressed in TECs,[8] we hypothesized that TECs are targets for AR-dependent actions on the thymus. Therefore, we generated E-ARKO mice using a K5-Cre construct[19] and mice with floxed AR exon 2. We bred the floxAR and K5-Cre strains with atherosclerosis-prone apoE⁻/⁻ mice and created E-ARKO apoE⁻/⁻ mice for studies of E-ARKO effects on atherosclerosis.

The ratio of AR exon 2 to exon 3 genomic DNA showed 58% reduction in sorted TECs from E-ARKO mice, whereas it was unaffected in enriched thymic CD3⁺ T cells (Figure 3A and 3B). Body weight and weights of androgen-sensitive organs (Figure IIA through IIC in the online-only Data Supplement), as well as serum testosterone (Figure 3C), were unchanged in E-ARKO.

Confirming our hypothesis, E-ARKO mice displayed increased thymic weight (Figure 3D); the effect was comparable with that found in castrated male apoE⁻/⁻ mice (Figure 2B).

Increased Atherosclerosis in E-ARKO Male Mice

In line with a disease-driving mechanism, the E-ARKO apoE⁻/⁻ mice displayed increased atherosclerosis (Figure 4A), which was more than doubled at 16 weeks of age (mean difference between E-ARKO and controls, 1.3×10^7 μm^2; 95% confidence interval, 0.3×10^7 to 2.4×10^7 μm^2). In the E-ARKO apoE⁻/⁻ mice, serum cholesterol or triglyceride levels were not significantly different from controls (Figure IID and IIE in the online-only Data Supplement). Analyzing other plaque composition variables in E-ARKO and control mice, we found no statistically significant differences in percentage collagen or neutral lipids or relative macrophage content of the plaque (Table I in the online-only Data Supplement).

To address the role of the thymus for the atherosclerosis phenotype of E-ARKO apoE⁻/⁻ mice, we subjected mice to thymectomy before puberty (at 3 weeks of age) and quantified atherosclerosis at 16 weeks of age (Figure 4B and 4C). Indeed, thymectomized E-ARKO mice showed no atherosclerosis phenotype (mean difference between E-ARKO and controls, 0.05×10^7 μm^2; 95% confidence interval, -0.5×10^7 to 0.5×10^7 μm^2). Further, thymectomy at this age did not per se affect the development of atherosclerosis in apoE⁻/⁻ mice (Figure III in the online-only Data Supplement). Thus, depletion of the AR in epithelial cells leads to increased atherosclerosis, which is dependent on the presence of the thymus.

We next studied T-cell infiltration in the vascular wall of E-ARKO mice. We performed immunohistochemistry of CD3⁺ T cells in aortic sections from E-ARKO and control mice and included in the panel anti-CD18 (expressed in most leukocyte subclasses) to visualize the leukocyte-dense plaque and anti-α-actin to visualize the vascular wall. The
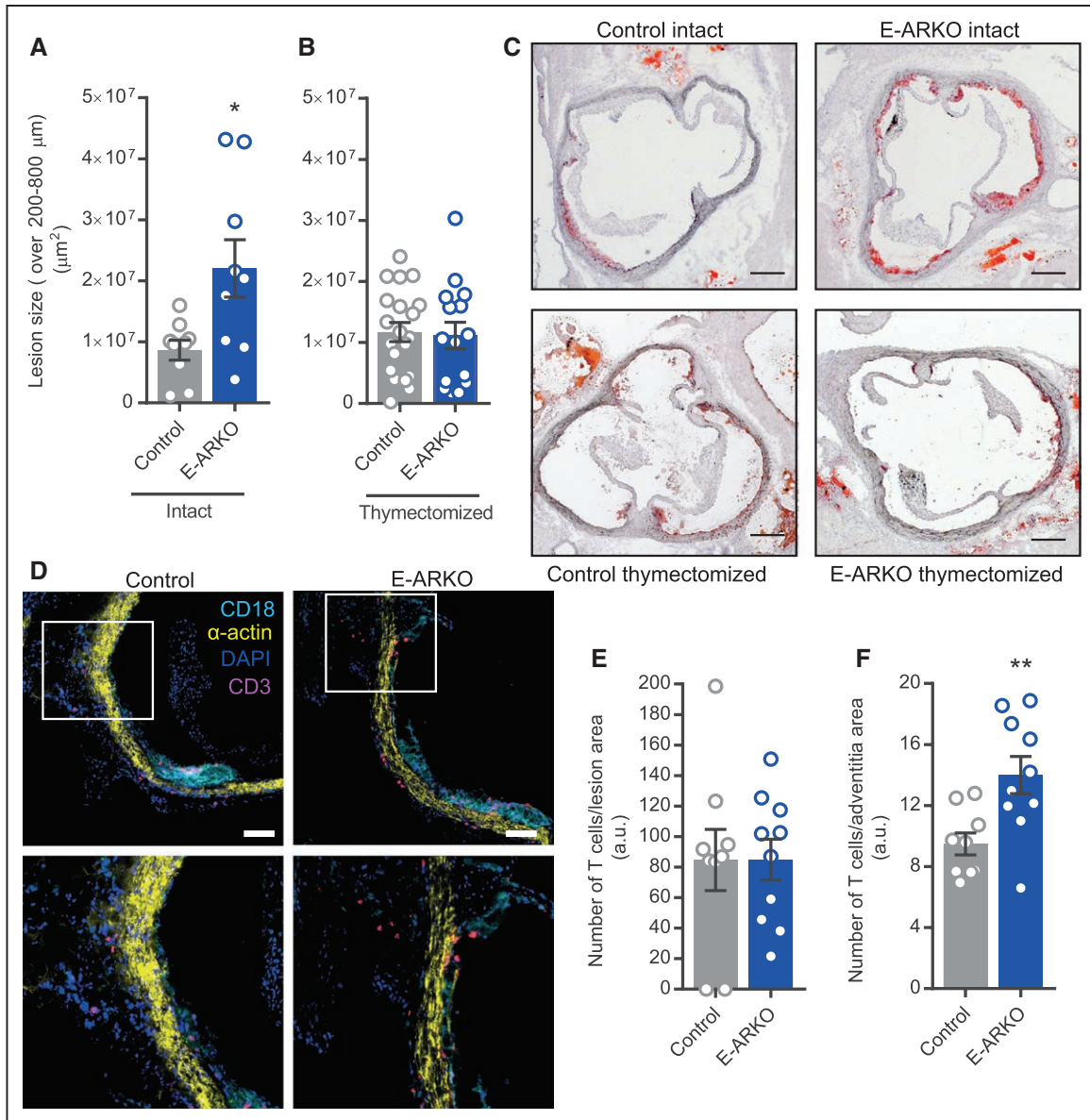
Figure 4. Increased atherosclerosis in E-ARKO (epithelial cell-specific AR knockout) male mice. **A** and **B**, Quantification of atherosclerotic lesion size in sections collected at 200, 400, 600, and 800 μm from the aortic cusps, of intact control (n=9) and E-ARKO (n=9) apoE^{−/−} mice (**A**) and from thymectomized control (n=20) and E-ARKO (n=15) apoE^{−/−} male mice (**B**) at 16 wk of age. The mice were fed a normal chow diet. *P<0.05 (Mann-Whitney *U* test). **C**, Representative pictures of Oil Red O staining of aortic root sections (scale bar=200 μm). **D**, Representative pictures of CD3 staining of aortic root sections from control and E-ARKO mice; CD3 (pink), smooth muscle α-actin (yellow), CD18 (cyan), nuclear stain (DAPI [4',6-diamidino-2-phenylindole], blue) (scale bar=100 μm). **Top**, Vessel media appear yellow, atherosclerotic lesions with dense CD18 staining appear cyan. **Bottom**, Magnification of area marked by a square in (**top**); staining of T cells (pink) in the vascular adventitia. **E** and **F**, Quantification of CD3+ T cell number in atherosclerotic lesions and adventitia in aortic root sections (1 section per mouse at 280 μm from the aortic cusps) from control (n=9) and E-ARKO (n=10) apoE^{−/−} mice. **P<0.01 (Student *t* test). Bars indicate means, error bars indicate SEM, and circles represent individual mice.

staining revealed that T cells were infiltrating the plaque but also to a large extent the vascular adventitia (examples shown in Figure 4D). Quantifying the number of T cells in different parts of the vascular wall, we found that the relative numbers of T cells were unchanged in the plaque but increased in the adventitia of E-ARKO mice (Figure 4E and 4F).

Discussion

Androgen deprivation therapy and castration of men with prostate cancer has been associated with increased risk of cardiovascular events.[3] In accordance, both castration and depletion of the AR increase atherosclerosis in male mice.[4] However, the target cell for the effect of testosterone/AR on atherosclerosis has remained unidentified.[16] Here, we report that the atheroprotective effect of testosterone in male mice is T-cell dependent and that depletion of the AR in epithelial cells results in increased thymus size and thymus-dependent atherosclerosis. Thus, our data suggest that the thymic epithelium is an important target compartment for the atheroprotective actions of testosterone.

Although there has been much focus on the role of T cells in atherogenesis,[5] the role of the thymus and thymic processes has

been surprisingly little studied. This may be because of the fact that the thymus has been considered by many to be unimportant in adult life.[24] The role of the thymus in T-cell homeostasis and T-cell–dependent disorders is indeed age dependent. Neonatal thymectomy affects the human peripheral T cell pool in an age-dependent manner[24] and is associated with increased frequencies of immune-related disorders.[25] Although thymectomy at 3 weeks of age accelerates autoimmune diabetes mellitus development in mice, thymectomy at 3 days or 6 weeks has no such effect.[26] Thus, both age at thymectomy and time since thymectomy affect its immunologic consequences. Thymectomy of neonatal mice has previously been reported to protect apoE$^{-/-}$ mice against atherosclerosis[27]; in our hands, thymectomy at 3 weeks of age did not per se alter the development of atherosclerosis. However, after thymectomy at 3 weeks, E-ARKO mice showed no atherosclerosis phenotype, suggesting that the older thymus may modulate atherogenesis in certain conditions. The neutral effect per se of thymectomy after the neonatal period may reflect its complex role in atherogenesis, such as seeding the peripheral immune system with both proatherogenic and atheroprotective T cell types.[5,28] Similarly, both pro- and antiatherogenic subtypes of T cells are deleted by an anti-CD3 antibody,[5] which may explain why this T-cell depletion regimen per se did not result in altered atherosclerosis burden in the present study. However, T-cell depletion abolished the effect of castration on atherosclerosis, paralleling the effects of thymectomy in E-ARKO.

There are several plausible mechanisms linking the AR in TECs to atherosclerosis: (1) because thymus size, which was increased in E-ARKO, is an important determinant of thymic output of T cells,[29] it is possible that an increased output of proatherogenic T cells to the periphery may increase vascular inflammation and thereby atherosclerosis. Of note, we found increased numbers of T cells in the vascular adventitia of E-ARKO mice—a compartment that also harbors the majority of T cells in human early atherosclerosis.[30] (2) Recent thymic emigrants, that is, immature T cells that derive from the thymus and continue their maturation to mature naive T cells in peripheral lymphoid organs,[31] may play a specific role in immune disorders beyond childhood,[31] in keeping with the importance of the adult thymus.[24,28] Although still incompletely mapped, certain properties of recent thymic emigrants, such as improved access to peripheral sites of inflammation, may potentially make them more proatherogenic than mature naive T cells[31–33] and may be highly relevant in an atherosclerosis setting. (3) Other thymic processes could also be implicated in the atherosclerosis phenotype of E-ARKO mice, as negative selection, formation of regulatory T cells, and other processes also are governed by TECs.[34] However, a general effect on negative selection processes may be less likely because it previously has been suggested to be unaltered in the E-ARKO model.[35] Further studies should decipher the nature of the connection between TEC function in general, and AR activation in TECs in particular, and atherogenesis.

Testosterone is the most important sex steroid hormone in males and plays a major role for male health and aging.[36] Prostate cancer is the most common form of cancer in men, and androgen-targeting treatment regimens have been associated with increased cardiovascular risk.[3] Indeed, cardiovascular disease rather than prostate cancer is the leading cause of death among men with prostate cancer,[37] highlighting the need for more specific

hormonal therapies. The development of selective AR modulators is ongoing[14] but requires increased background understanding of the specific target cells of androgens. Therefore, identification of the androgen target cell(s) for the protection from atherosclerosis can have major future clinical implications.

In conclusion, we show that atherogenesis induced by testosterone deficiency or abrogation of AR is thymus- and T-cell–dependent in male mice and that the TEC is a likely target cell for the antiatherogenic actions of testosterone. These insights may pave the way for new therapeutic strategies for safer endocrine treatment of prostate cancer.

Disclosures

None.

References

1. Kelly DM, Jones TH. Testosterone: a vascular hormone in health and disease. *J Endocrinol*. 2013;217:R47–R71. doi: 10.1530/JOE-12-0582.
2. Ohlsson C, Barrett-Connor E, Bhasin S, Orwoll E, Labrie F, Karlsson MK, Ljunggren O, Vandenput L, Mellström D, Tivesten A. High serum testosterone is associated with reduced risk of cardiovascular events in elderly men. The MrOS (Osteoporotic Fractures in Men) study in Sweden. *J Am Coll Cardiol*. 2011;58:1674–1681. doi: 10.1016/j.jacc.2011.07.019.
3. Tivesten Å, Pinthus JH, Clarke N, Duivenvoorden W, Nilsson J. Cardiovascular risk with androgen deprivation therapy for prostate cancer: potential mechanisms. *Urol Oncol*. 2015;33:464–475. doi: 10.1016/j.urolonc.2015.05.030.
4. Bourghardt J, Wilhelmson AS, Alexanderson C, De Gendt K, Verhoeven G, Krettek A, Ohlsson C, Tivesten A. Androgen receptor-dependent and independent atheroprotection by testosterone in male mice. *Endocrinology*. 2010;151:5428–5437. doi: 10.1210/en.2010-0663.
5. Ketelhuth DF, Hansson GK. Adaptive response of T and B cells in atherosclerosis. *Circ Res*. 2016;118:668–678. doi: 10.1161/CIRCRESAHA.115.306427.
6. Libby P, Lichtman AH, Hansson GK. Immune effector mechanisms implicated in atherosclerosis: from mice to humans. *Immunity*. 2013;38:1092–1104. doi: 10.1016/j.immuni.2013.06.009.
7. Ridker PM, Everett BM, Thuren T, et al; CANTOS Trial Group. Antiinflammatory therapy with canakinumab for atherosclerotic disease. *N Engl J Med*. 2017;377:1119–1131. doi: 10.1056/NEJMoa1707914.
8. Olsen NJ, Olson G, Viselli SM, Gu X, Kovacs WJ. Androgen receptors in thymic epithelium modulate thymus size and thymocyte development. *Endocrinology*. 2001;142:1278–1283. doi: 10.1210/endo.142.3.8032.
9. Roden AC, Moser MT, Tri SD, Mercader M, Kuntz SM, Dong H, Hurwitz AA, McKean DJ, Celis E, Leibovich BC, Allison JP, Kwon ED. Augmentation of t cell levels and responses induced by androgen deprivation. *J Immunol*. 2004;173:6098–6108.
10. Heng TS, Goldberg GL, Gray DH, Sutherland JS, Chidgey AP, Boyd RL. Effects of castration on thymocyte development in two different models of thymic involution. *J Immunol*. 2005;175:2982–2993.
11. Sutherland JS, Goldberg GL, Hammett MV, Uldrich AP, Berzins SP, Heng TS, Blazar BR, Millar JL, Malin MA, Chidgey AP, Boyd RL. Activation of thymic regeneration in mice and humans following androgen blockade. *J Immunol*. 2005;175:2741–2753.

12. Kelly RM, Highfill SL, Panoskaltsis-Mortari A, Taylor PA, Boyd RL, Holländer GA, Blazar BR. Keratinocyte growth factor and androgen blockade work in concert to protect against conditioning regimen-induced thymic epithelial damage and enhance T-cell reconstitution after murine bone marrow transplantation. *Blood*. 2008;111:5734–5744. doi: 10.1182/blood-2008-01-136531.

13. Williams KM, Lucas PJ, Bare CV, Wang J, Chu YW, Tayler E, Kapoor V, Gress RE. CCL25 increases thymopoiesis after androgen withdrawal. *Blood*. 2008;112:3255–3263. doi: 10.1182/blood-2008-04-153627.

14. Narayanan R, Coss CC, Dalton JT. Development of selective androgen receptor modulators (SARMs). *Mol Cell Endocrinol*. 2018;465:134–142. doi: 10.1016/j.mce.2017.06.013.

15. Takov K, Wu J, Denvir MA, Smith LB, Hadoke PWF. The role of androgen receptors in atherosclerosis. *Mol Cell Endocrinol*. 2018;465:82–91. doi: 10.1016/j.mce.2017.10.006.

16. Huang CK, Pang H, Wang L, Niu Y, Luo J, Chang E, Sparks JD, Lee SO, Chang C. New therapy via targeting androgen receptor in monocytes/macrophages to battle atherosclerosis. *Hypertension*. 2014;63:1345–1353. doi: 10.1161/HYPERTENSIONAHA.113.02804.

17. Calderón L, Boehm T. Synergistic, context-dependent, and hierarchical functions of epithelial components in thymic microenvironments. *Cell*. 2012;149:159–172. doi: 10.1016/j.cell.2012.01.049.

18. De Gendt K, Swinnen JV, Saunders PT, Schoonjans L, Dewerchin M, Devos A, Tan K, Atanassova N, Claessens F, Lécureuil C, Heyns W, Carmeliet P, Guillou F, Sharpe RM, Verhoeven G. A Sertoli cell-selective knockout of the androgen receptor causes spermatogenic arrest in meiosis. *Proc Natl Acad Sci USA*. 2004;101:1327–1332. doi: 10.1073/pnas.0308114100.

19. Ramírez A, Bravo A, Jorcano JL, Vidal M. Sequences 5' of the bovine keratin 5 gene direct tissue- and cell-type-specific expression of a lacZ gene in the adult and during development. *Differentiation*. 1994;58:53–64. doi: 10.1046/j.1432-0436.1994.5810053.x.

20. Daugherty A, Tall AR, Daemen MJAP, Falk E, Fisher EA, García-Cardeña G, Lusis AJ, Owens AP III, Rosenfeld ME, Virmani R; American Heart Association Council on Arteriosclerosis, Thrombosis and Vascular Biology; Council on Basic Cardiovascular Sciences. Recommendation on design, execution, and reporting of animal atherosclerosis studies: a scientific statement from the American Heart Association. *Arterioscler Thromb Vasc Biol*. 2017;37:e131–e157. doi: 10.1161/ATV.0000000000000062.

21. Kita T, Yamashita T, Sasaki N, Kasahara K, Sasaki Y, Yodoi K, Takeda M, Nakajima K, Hirata K. Regression of atherosclerosis with anti-CD3 antibody via augmenting a regulatory T-cell response in mice. *Cardiovasc Res*. 2014;102:107–117. doi: 10.1093/cvr/cvu002.

22. Livak KJ, Schmittgen TD. Analysis of relative gene expression data using real-time quantitative PCR and the 2(-Delta Delta C(T)) Method. *Methods*. 2001;25:402–408. doi: 10.1006/meth.2001.1262.

23. Nilsson ME, Vandenput L, Tivesten Å, Norlén AK, Lagerquist MK, Windahl SH, Börjesson AE, Farman HH, Poutanen M, Benrick A, Maliqueo M, Stener-Victorin E, Ryberg H, Ohlsson C. Measurement of a comprehensive sex steroid profile in rodent serum by high-sensitive gas chromatography-tandem mass spectrometry. *Endocrinology*. 2015;156:2492–2502. doi: 10.1210/en.2014-1890.

24. van den Broek T, Delemarre EM, Janssen WJ, Nievelstein RA, Broen JC, Tesselaar K, Borghans JA, Nieuwenhuis EE, Prakken BJ, Mokry M, Jansen NJ, van Wijk F. Neonatal thymectomy reveals differentiation and plasticity within human naive T cells. *J Clin Invest*. 2016;126:1126–1136. doi: 10.1172/JCI84997.

25. Gudmundsdottir J, Soderling J, Berggren H, Oskarsdottir S, Neovius M, Stephansson O, Ekwall O. Long-term clinical effects of early thymectomy: associations with autoimmune diseases, cancer, infections, and atopic diseases [published online ahead of print February 14, 2018]. *J Allergy Clin Immunol*. doi: 10.1016/j.jaci.2018.01.037. https://www.sciencedirect.com/science/article/pii/S0091674918302288?via%3Dihub.

26. Gagnerault MC, Lanvin O, Pasquier V, Garcia C, Damotte D, Lucas B, Lepault F. Autoimmunity during thymectomy-induced lymphopenia: role of thymus ablation and initial effector T cell activation timing in nonobese diabetic mice. *J Immunol*. 2009;183:4913–4920. doi: 10.4049/jimmunol.0901954.

27. To K, Agrotis A, Besra G, Bobik A, Toh BH. NKT cell subsets mediate differential proatherogenic effects in ApoE-/- mice. *Arterioscler Thromb Vasc Biol*. 2009;29:671–677. doi: 10.1161/ATVBAHA.108.182592.

28. Vrisekoop N, den Braber I, de Boer AB, Ruiter AF, Ackermans MT, van der Crabben SN, Schrijver EH, Spierenburg G, Sauerwein HP, Hazenberg MD, de Boer RJ, Miedema F, Borghans JA, Tesselaar K. Sparse production but preferential incorporation of recently produced naive T cells in the human peripheral pool. *Proc Natl Acad Sci USA*. 2008;105:6115–6120. doi: 10.1073/pnas.0709713105.

29. Hale JS, Boursalian TE, Turk GL, Fink PJ. Thymic output in aged mice. *Proc Natl Acad Sci USA*. 2006;103:8447–8452. doi: 10.1073/pnas.0601040103.

30. van Dijk RA, Duinisveld AJ, Schaapherder AF, Mulder-Stapel A, Hamming JF, Kuiper J, de Boer OJ, van der Wal AC, Kolodgie FD, Virmani R, Lindeman JH. A change in inflammatory footprint precedes plaque instability: a systematic evaluation of cellular aspects of the adaptive immune response in human atherosclerosis. *J Am Heart Assoc*. 2015;4:e001403.

31. Fink PJ. The biology of recent thymic emigrants. *Annu Rev Immunol*. 2013;31:31–50. doi: 10.1146/annurev-immunol-032712-100010.

32. Berkley AM, Fink PJ. Cutting edge: CD8+ recent thymic emigrants exhibit increased responses to low-affinity ligands and improved access to peripheral sites of inflammation. *J Immunol*. 2014;193:3262–3266. doi: 10.4049/jimmunol.1401870.

33. Friesen TJ, Ji Q, Fink PJ. Recent thymic emigrants are tolerized in the absence of inflammation. *J Exp Med*. 2016;213:913–920. doi: 10.1084/jem.20151990.

34. Klein L, Kyewski B, Allen PM, Hogquist KA. Positive and negative selection of the T cell repertoire: what thymocytes see (and don't see). *Nat Rev Immunol*. 2014;14:377–391. doi: 10.1038/nri3667.

35. Lai KP, Lai JJ, Chang P, Altuwaijri S, Hsu JW, Chuang KH, Shyr CR, Yeh S, Chang C. Targeting thymic epithelia AR enhances T-cell reconstitution and bone marrow transplant grafting efficacy. *Mol Endocrinol*. 2013;27:25–37. doi: 10.1210/me.2012-1244.

36. Kaufman JM, Vermeulen A. The decline of androgen levels in elderly men and its clinical and therapeutic implications. *Endocr Rev*. 2005;26:833–876. doi: 10.1210/er.2004-0013.

37. Ketchandji M, Kuo YF, Shahinian VB, Goodwin JS. Cause of death in older men after the diagnosis of prostate cancer. *J Am Geriatr Soc*. 2009;57:24–30. doi: 10.1111/j.1532-5415.2008.02091.x.

Highlights

- Testosterone deficiency induced by prepubertal castration of male apoE$^{-/-}$ mice increased atherosclerotic lesion area. Depletion of T cells using an anti-CD3 antibody abolished castration-induced atherogenesis, demonstrating a role of T cells.
- Male mice with depletion of the AR (androgen receptor—the receptor for testosterone) specifically in epithelial cells (E-ARKO [epithelial cell–specific AR knockout] mice) showed increased thymus weight, comparable with that of castrated mice. E-ARKO mice on an apoE$^{-/-}$ background displayed significantly increased atherosclerosis, which was absent in mice subjected to prepubertal thymectomy.
- In summary, we show that atherogenesis induced by testosterone/AR deficiency is thymus- and T-cell–dependent in male mice and that the thymic epithelial cell is a likely target cell for the antiatherogenic actions of testosterone.
- These insights may pave the way for new therapeutic strategies for safer endocrine treatment of prostate cancer.